CHIN. PHYS. LETT. Vol. 38, No. 8 (2021) 085202

Synergistic Influences of Kinetic Effects from Thermal Particles and Fast Ions on Internal Kink Mode

Yutian Miao(苗雨田)[1,2], G. Z. Hao(郝广周)[2*], Yue Liu(刘悦)[1*], H. D. He(何宏达)[2], W. Chen(陈伟)[2], Y. Q. Wang(王雍钦)[2], A. K. Wang(王爱科)[2], and M. Xu(许敏)[2]

[1]*Key Laboratory of Materials Modification by Laser, Ion, and Electron Beams (Ministry of Education), School of Physics, Dalian University of Technology, Dalian 116024, China*
[2]*Southwestern Institute of Physics, Chengdu 610041, China*

(Received 8 April 2021; accepted 13 July 2021; published online 2 August 2021)

The kinetic effects of thermal particles and fast ions on internal kink (IK) mode are numerically investigated by the MHD-kinetic hybrid code MARS-K. It is shown that either thermal particles or fast ions have stabilizing influence on IK. However, the former can not fully stabilize IK, and the later can suppress the IK. In addition, the synergistic effect from thermal particles and fast ions induces more stronger damping on IK. The kinetic effects from particles significantly raise the critical value of poloidal beta ($\beta_{\rm p}^{\rm crit}$) for driving IK in the toroidal plasma. This implies a method of controlling IK or sawtooth in the high-$\beta_{\rm p}$ discharge scenario of tokamak. It is noted that, at the $q = 1$ rational surface, mode structure becomes more sharp due to the self-consistent modification by particles' kinetic effect.

DOI: 10.1088/0256-307X/38/8/085202

Sawtooth oscillations have been observed in various tokamak devices. It is indicated by the periodic relaxation oscillations of the plasma temperature, density and other plasma parameters in the central region, when the safety factor at magnetic axis (q_0) drops below unity.[1] While it is generally caused by internal kink mode with helicity $m/n = 1$ (m and n are the poloidal and toroidal mode numbers, respectively). Sawtooth crash results in the redistribution of energetic particles and the reduce of plasma performance. It is possible that sawteeth supplies the magnetic island seed to initiate the growth of neoclassical tearing modes (NTMs), which can also reduce plasma performance and even lead to plasma disruptions. Since the internal kink mode is responsible for sawtooth activities, the mechanism of controlling internal kink mode is required for the high-current discharge of tokamak, such as ITER 15 MA scenario.

Internal kink was firstly theoretically predicted in a cylindrical pinch using the ideal magnetohydrodynamic (MHD) model, showing that the mode can be driven by both pressure and current.[2] Bussac *et al.* found that the internal kink mode can be stable when the poloidal beta $\beta_{\rm p}$ is smaller than a critical value in a toroidal plasma.[3] Plasma resistivity destabilizes the internal kink mode.[4,5]

Previous studies have shown that the internal kink is fully suppressed by the kinetic effects from fast ions,[6–9] while a so-called fishbone mode is excited as the fast ions' beta exceeds a threshold value.[10–17] Moreover, the kinetic effects from thermal particles modify the inertia and the perturbed potential energy of the MHD mode,[18] and also modify the the threshold value for driving fishbone mode.[19] However, the kinetic effect of thermal particles on the internal kink (IK) mode requires further investigations. Therefore, in this work, we carry out this kind of study, and investigate the synergistic influence of thermal and fast particles on IK.

In this Letter, we first introduce the model implemented in MARS-K code. The equilibrium used is presented. Then, numerical results and discussions are given. Finally, we provide the conclusions.

MHD-Kinetic Hybrid Formulation. In this work, the MHD-kinetic hybrid code MARS-K is employed, which self-consistently solves the linearized single fluid MHD equations.[20] The kinetic effects enter into the momentum equation via the perturbed kinetic pressure tensor as follows:

$$\delta \boldsymbol{p} = p_{\parallel}\hat{\boldsymbol{b}}\hat{\boldsymbol{b}} + p_{\perp}(\boldsymbol{I} - \hat{\boldsymbol{b}}\hat{\boldsymbol{b}}), \tag{1}$$

$$p_{\parallel} = p_{\parallel}^{\rm a} + \alpha^{\rm NTB_i} p_{\parallel}^{\rm na,NTB_i} + \sum_{j={\rm i,e,h}} \alpha^{{\rm NTD}_j} p_{\parallel}^{{\rm na,NTD}_j}, \tag{2}$$

$$p_{\perp} = p_{\perp}^{\rm a} + \alpha^{\rm NTB_i} p_{\perp}^{\rm na,NTB_i} + \sum_{j={\rm i,e,h}} \alpha^{{\rm NTD}_j} p_{\perp}^{{\rm na,NTD}_j}, \tag{3}$$

where $p_{\parallel}$ and $p_{\perp}$ are the parallel and perpendicular components of the pressure perturbations, respectively. Each component of the perturbed pressure involves both adiabatic (superscript a) and non-

Supported by the National Key R&D Program of China (Grant No. 2019YFE03050003), the National Magnetic Confinement Fusion Science Program (Grant No. 2018YFE0304103), and the National Natural Science Foundation of China (Grant Nos. 11775067 and 11905067).
*Corresponding authors. Email:haogz@swip.ac.cn; liuyue@dlut.edu.cn
© 2021 Chinese Physical Society and IOP Publishing Ltd

adiabatic (superscript na) parts; $\hat{\boldsymbol{b}} \equiv \boldsymbol{B}/B$ with $B = |\boldsymbol{B}|$. Here α^{NTD_j} is multiplier for the non-adiabatic contribution (also called kinetic effect here) which is induced by toroidal precession drift resonance (superscript NTD) of trapped particles; $\alpha^{\mathrm{NTB_i}}$ is the one for denoting bounce resonance (superscript NTB) of trapped thermal ions. The bounce frequencies of thermal electrons and fast ions are far away from the mode frequency studied in this work. Hence, the related bounce resonances are not included in this work. The subscripts $j = i, e$ and h denote thermal ions, thermal electrons and fast ions, respectively; $\alpha^{\mathrm{NTD}_j} = 0$ and $\alpha^{\mathrm{NTB_i}} = 0$ stand for that the corresponding kinetic effects are not considered, while $\alpha^{\mathrm{NTD}_j} = 1$ and $\alpha^{\mathrm{NTB_i}} = 1$ stand for that all the mentioned kinetic effects are included.

The procedure of perturbed kinetic pressure tensor was stated in Ref. [21]. Without referring to details, here we only show the wave-particle resonance operator λ, which is the key factor of the drift kinetic physics,

$$\lambda = \frac{n[\omega_{*N} + (\hat{\epsilon}_k - 3/2)\omega_{*T} + \omega_{\mathrm{E}}] - \tilde{\omega}}{n\omega_{\mathrm{d}} + [\sigma(m + nq) + l]\omega_{\mathrm{b}} + n\omega_{\mathrm{E}} - i\nu_{\mathrm{eff}} - \tilde{\omega}}, \quad (4)$$

where $\omega_{*N} = \sigma_1 \frac{\rho_{\mathrm{L}}}{r} \frac{v_{\mathrm{th}}}{R_0} \frac{1}{4\varepsilon} (\frac{-r}{N} \frac{dN}{dR})$ and $\omega_{*T} = \sigma_1 \frac{\rho_{\mathrm{L}}}{r} \frac{v_{\mathrm{th}}}{R_0} \frac{1}{4\varepsilon} (\frac{-r}{T} \frac{dT}{dR})$ are the diamagnetic drift frequencies due to the particles' density and temperature gradients, respectively; $v_{\mathrm{th}} \equiv \sqrt{2T/M}$ and $\rho_{\mathrm{L}} \equiv \sqrt{v_{\mathrm{th}}/\omega_c}$ are the thermal velocity and Larmor radius of particle, respectively. N, M and T are the density, particle mass, and temperature, respectively; $\omega_c \equiv eB_0/M$ is the gyro-frequency of the particle with B_0 being the equilibrium magnetic field; $\sigma_1 = 1$ and $\sigma_1 = -1$ stand for ions and electrons, respectively; $\hat{\epsilon}_k \equiv \epsilon_k/k$ is the particle kinetic energy normalized by the corresponding particles' temperature; ω_{E} is the $\boldsymbol{E} \times \boldsymbol{B}$ drift frequency due to the equilibrium electrostatic potential. (We point out that our hybrid formulation is partly based on the standard single fluid description of the plasma. The toroidal rotation frequency of plasma represents the bulk ion rotation, which is actually the sum of the ω_{E} is the $\boldsymbol{E} \times \boldsymbol{B}$ flow, the bulk ion diamagnetic flow and the part driven by external momentum source. These flows are not separable in the single fluid description). For simplicity, ω_{E} in the kinetic pressure tensor is assumed to be identical to that in the inertial term in our work here; m and n are the poloidal and toroidal mode numbers, respectively; q is the safety factor; l is the harmonic number during the decomposition in Fourier series; ω_{d} is the bounce-orbit-averaged toroidal precession drift frequency of trapped particles. For trapped particles, $\sigma = 0$, and ω_{b} is the bounce frequency. For passing particles, $\sigma = 1$, and ω_{b} represents the transit frequency. Here ν_{eff} is the collision frequency associated with a simple Krook collision model[22] in our numerical simulation; $\tilde{\omega}$ is a complex number which represents the mode eigenvalue. The resonance factor depends on the plasma rotation frequency, particle's frequencies, collisionality rate, as well as the mode eigenvalue. We emphasize that the mode eigenvalue enters into Eq. (4) via $\tilde{\omega} = i\gamma + \omega_r$ with γ being the mode growth rate and ω_r being the mode frequency in laboratory frame. Normally, for low-frequency instability, the mode frequency is easily matched by the toroidal precession drift frequency of trapped fast ions, which in turn induces the wave-particle resonance.

Simulation Setup. In the present work, a circular cross-section tokamak with inverse aspect ratio ($\epsilon = a/R_0 = 0.36/1.65 \simeq 0.2$) is assumed. The toroidal magnetic field at axis is $B_0 = 1.3\,\mathrm{T}$, the on-axis electron density, temperature and thermal ion temperature are assumed to be $n_{\mathrm{e}}(0) = 4.73 \times 10^{19}\,\mathrm{m}^{-3}$, $T_{\mathrm{e}}(0) = 1.0\,\mathrm{keV}$ and $T_i(0) = 1.2\,\mathrm{keV}$, respectively. In our simulation, the neutrality condition is guaranteed. In other words, the electron density equals the summation of thermal and fast ion density. The above parameters are comparable with those for the discharges on the HL-2A device.[23]

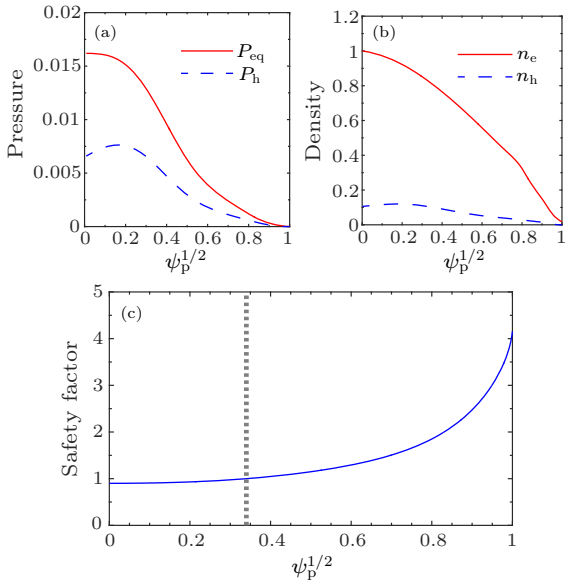

Fig. 1. Radial profiles of (a) plasma equilibrium pressure (solid) and fast ion pressure (dashed), (b) electron density (solid) and fast ion density (dashed), (c) safety factor q. The vertical line denotes the location of the $q = 1$ rational surface which is about 0.34; ψ_{p} is the normalized equilibrium poloidal flux.

The radial profiles of the normalized equilibrium and fast ion pressure are displayed in Fig. 1(a). The ratio of fast ion pressure (P_{h}) to total plasma pressure (P_{eq}) is about 40% in the core region. The plasma equilibrium pressure is normalized by B_0^2/μ_0 with $\beta_N = 1.67$. The normalized density profiles of electron and fast ion are shown in Fig. 1(b). The ratio of fast ion density (n_{h}) to electron one (n_{e}) is about 10% at the axis. Here, the electron density is normal-

ized to unity at the magnetic axis. The safety factor q profile is displayed in Fig. 1(c), with the on-axis value $q_0 = 0.90$ and the edge value $q_a = 4.15$, which allows the existence of internal kink instability in MHD frame.

Simulation Results and Discussions—Particles' Frequencies. Since the mode-particle resonance is one of key elements to study the drift kinetic physics, we present the radial distribution of particles' frequencies in Fig. 2. The frequencies are normalized by the on-axis Alfvén frequency [$\omega_A \equiv B_0/(R_0\sqrt{\mu_0\rho_0})$, where ρ_0 is plasma mass density], and averaged over the particle velocity space as well as over the flux surface. It is shown that the toroidal precession drift frequency of fast ions (yellow) is roughly equal to the bounce frequency of thermal ions (green), which is about 7×10^{-3} at the position of $q = 1$ [i.e., $\sqrt{(\psi_p)} = 0.34$]. The toroidal precession drift frequencies of thermal ions (red) and electrons (blue) have the same value but opposite directions.

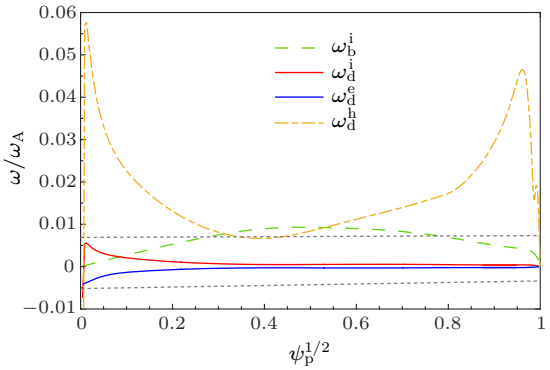

Fig. 2. The radial profiles of particles' frequencies with parameters ω_b^i: bounce frequency of thermal ion, ω_d^i: toroidal precession drift frequency of trapped thermal ion, ω_d^e: toroidal precession drift frequency of trapped thermal electron, ω_d^h: toroidal precession drift frequency of trapped fast ion. The dotted horizontal lines represent the range of the mode real frequency simulated in this work that matches the particle frequency.

Kinetic Effects on Mode Eigenvalue. Recently, the kinetic effects from thermal particles on the stability of internal kink mode have been studied,[24] where the fast ion contribution was not considered. In this work, we numerically investigate the synergistic influences from thermal particles and fast ions on internal kink instability.

In MARS-K, the contributions induced by different kinds of particle motions can be separately controlled. This allows us using MARS-K to investigate the combined effects of various kinds of kinetic contributions on the internal kink instability.[25] The terms $\mathrm{NTD_i}$, $\mathrm{NTD_e}$, $\mathrm{NTD_h}$ and $\mathrm{NTB_i}$ mentioned below represent the non-adiabatic effect from precession motion of trapped thermal ions, thermal electrons, fast ions and from bounce motion of trapped thermal ions, respectively.

As shown in Fig. 3, five cases are studied: (i) non-adiabatic contribution only from the toroidal precession drift resonance of thermal electron (i.e. only $\mathrm{NTD_e}$ is considered, as plotted by blue curve in Fig. 3); (ii) only $\mathrm{NTD_i}$ (red); (iii) only $\mathrm{NTD_h}$ (purple); (iv) the case of including $\mathrm{NTD_e}$, $\mathrm{NTD_i}$ and $\mathrm{NTD_h}$ (green); (v) the case of including $\mathrm{NTD_e}$, $\mathrm{NTD_i}$, $\mathrm{NTD_h}$ and $\mathrm{NTB_i}$ (yellow).

Obviously, the mode can not be fully stabilized for the case of only including $\mathrm{NTD_i}$ or $\mathrm{NTD_e}$. Here, the cases of only $\mathrm{NTD_i}$ and only $\mathrm{NTD_e}$ result in an almost anti-symmetry in the mode real frequency as expected. This is due to that ω_d^i and ω_d^e (with the same particle energy and pitch angle) have the opposite direction, while they have the same magnitude.

In comparison, the stabilization effect from trapped fast ions is much stronger than that from thermal particles, and result in the full suppression of internal kink when $\alpha^{\mathrm{NTD_h}}$ exceeds a critical value $\alpha^{\mathrm{NTD_{h,c}}}$. When the thermal particle kinetic effect is included at the same time, $\alpha^{\mathrm{NTD_{h,c}}}$ for suppressing internal kink is significantly reduced. Furthermore, the kinetic effect from bounce motion of thermal ions induce further decrease of $\alpha^{\mathrm{NTD_{h,c}}}$, whose critical value is about 0.2, smaller than the case represented by the green curve ($\alpha^{\mathrm{NTD_{h,c}}} \approx 0.4$). It is clearly indicated that the synergistic influence of thermal particles and fast ions can supply much stronger damping on the mode, compared with the individual cases.

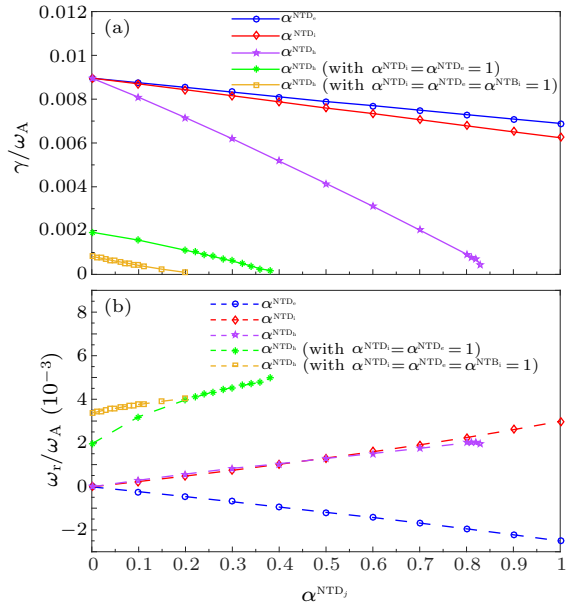

Fig. 3. The mode growth rate (a) and frequency (b) versus different kinetic effects for the equilibrium given in Fig. 1. As a function of scaling factor α^{NTD_j} for non-adiabatic contribution of trapped particles (see main text).

For the convenient of discussing the numerical results, the perturbed kinetic energy from particles δW_K is introduced and written as $\delta W_K = \alpha^{\mathrm{NTB_i}}\delta W_K^{\mathrm{na,NTB_i}} + \sum_{j=\mathrm{i,e,h}} \alpha^{\mathrm{NTD}_j}\delta W_K^{\mathrm{na,NTD}_j}$, the

components of $\delta\hat{W}_{\rm K}$ are plotted in Fig. 4, for different chooses of fast ion parameter $\alpha^{\rm NTD_h}$ for case v in Fig. 3. For the real part of the perturbed energy ${\rm Re}(\delta\hat{W}_{\rm K})$, Fig. 4(a) shows that the contribution mainly comes from ${\rm NTD_e}$. With increasing ${\rm NTD_h}$, the contributions from ${\rm NTB_i}$ and ${\rm NTD_e}$ are increased. While, due to the decrease of the component related to ${\rm NTD_i}$, the total value of ${\rm Re}(\delta\hat{W}_{\rm K})$ has a slight drop with increasing ${\rm NTD_h}$. In Fig. 4(b), the total value of imaginary part ${\rm Im}(\delta\hat{W}_{\rm K})$ increases with increasing ${\rm NTD_h}$. Although the contributions from ${\rm NTB_i}$ and ${\rm NTD_e}$ partially cancel the contributions from ${\rm NTD_i}$ and ${\rm NTD_h}$, the contribution from ${\rm NTD_i}$ is dominant to the total value. Here, we point out that the weight factors for thermal particles (i.e. $\alpha^{\rm NTB_i}$, $\alpha^{\rm NTD_i}$ and $\alpha^{\rm NTD_e}$) are unit, which is much larger than that for fast ions (i.e. $\alpha^{\rm NTD_h} = 0.1$). In other words, if $\alpha^{\rm NTD_h} = 1.0$, the fast ion contribution should be comparable with that from thermal particles. Hence, both thermal particles and fast ions have the important contribution for internal kink stabilization in the synergistic case as studied above.

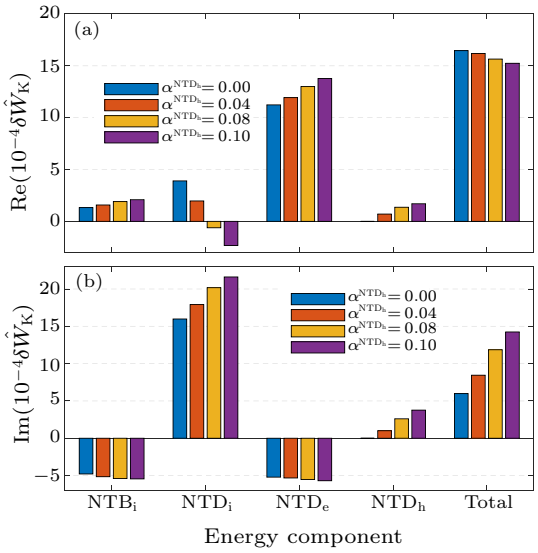

Fig. 4. Detailed perturbed energy components induced by particles for the real (a) and imaginary (b) parts of $\delta\hat{W}_{\rm K}$. Four cases with $\alpha^{\rm NTD_i} = \alpha^{\rm NTD_e} = \alpha^{\rm NTB_i} = 1$ are simulated.

As discussed in Ref. [19], for the self-consistent computations, the IK instability satisfies the general dispersion relation. The normalized version of the general dispersion relation can be rewritten as $\omega_r^2 - \gamma^2 = {\rm Re}(\delta\hat{W}_{\rm MHD} + \delta\hat{W}_{\rm K})$ and $2\omega_r\gamma = {\rm Im}(\delta\hat{W}_{\rm MHD} + \delta\hat{W}_{\rm K})$. Clearly, the term $\omega_r^2 - \gamma^2$ is exactly linearly propositional to ${\rm Re}(\delta\hat{W}_{\rm MHD} + \delta\hat{W}_{\rm K})$, similarly, $2\omega_r\gamma$ linearly depends on ${\rm Im}(\delta\hat{W}_{\rm MHD} + \delta\hat{W}_{\rm K})$. However, either the mode frequency (ω_r) or the growth rate (γ) depends on both ${\rm Re}(\delta\hat{W}_{\rm MHD})$ and ${\rm Re}(\delta\hat{W}_{\rm K})$, ${\rm Im}(\delta\hat{W}_{\rm MHD})$ and ${\rm Im}(\delta\hat{W}_{\rm K})$, when ω_r is comparable to γ. Only if the mode near the marginal points (i.e. $\omega_r \gg \gamma >\sim 0$), it can imply a relation $\omega_r \simeq \sqrt{{\rm Re}(\delta\hat{W}_{\rm MHD} + \delta\hat{W}_{\rm K})}$, $\gamma \simeq \sqrt{{\rm Im}(\delta\hat{W}_{\rm MHD} + \delta\hat{W}_{\rm K})}$.

Kinetic Effects on Mode Structure. The radial mode structures of internal kink instability for the studied cases in Fig. 3 are shown in Fig. 5. The black line displays the mode structure of the fluid internal kink perturbation, which is similar to the flat-top function as usually used in the theoretical studies.[10,12,26] However, when the kinetic effect is included as carried out in this work, the particles have the significant modification on the mode structures. Especially, the kinetic internal kink becomes more sharp at $q = 1$ rational surface, due to the strong wave-particle resonance. In addition, the mode structure has a drop at the core region. The drop amplitude is related to the particle species and the associated kinetic contributions.

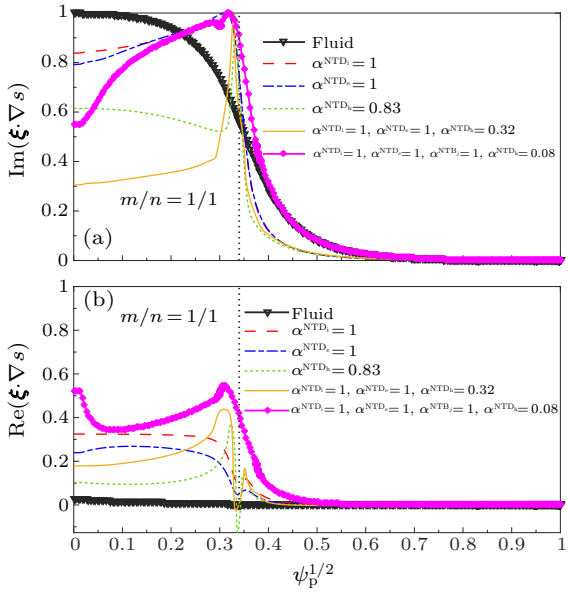

Fig. 5. The imaginary (a) and real (b) parts of radial displacement of internal kink corresponding to the cases studied in Fig. 3. The dashed vertical line denotes the location of the $q = 1$ rational surface. For each case, displacement is separately normalized by the maximum in $[{\rm Re}(\boldsymbol{\xi}\cdot\nabla s), {\rm Im}(\boldsymbol{\xi}\cdot\nabla s)]$.

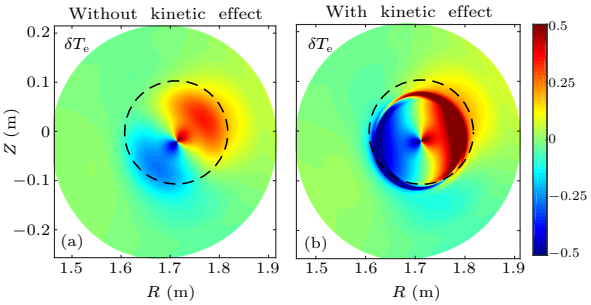

Fig. 6. Contour plot of perturbed temperature ($\delta T_{\rm e}$) (a) without and (b) with kinetic effect. The dashed circle denotes the $q = 1$ rational surface. Here, $\delta T_{\rm e}$ is estimated based on the formula $\delta T_{\rm e} = \boldsymbol{\xi}\cdot\nabla T_{\rm e}$.

Furthermore, the 2D plot of the mode structure (in terms of δT_e) is shown in Fig. 6, which allows the possibility of direct comparison between simulations and experimental data measured by electron cyclotron emission image (ECEI). Without kinetic effect [Fig. 6(a)], the perturbation is localized inside the $q = 1$ rational surface (dashed line). The perturbations in strong field side is slightly smaller than that in the weak field side. However, with the kinetic effects [Fig. 6(b)], the structure becomes twisted and the maximum value moves outward to the $q = 1$ rational surface.

Kinetic Effects on Poloidal Beta. This work also presents a systematic investigation of influence of various kinetic effects on critical poloidal beta (β_p^{crit}) for driving internal kink in toroidal plasma. An interesting result is shown in Fig. 7, when β_p exceeds a critical value (β_p^{crit}), internal kink instability can be triggered, and the mode growth rate rapidly grows with increasing β_p. The value of β_p^{crit} for fluid case (black) is about 0.33, which is consistent with the theoretical prediction.[3] The plasma flow (cyan) almost does not affect the mode instability rate, but results in the increase of the mode real frequency. If the kinetic effects of NTD_i (red) or NTD_e (blue) are taken into account individually, mode instability is reduced and the mode real frequency appears anti-symmetric, but the value of β_p^{crit} stays the same as the fluid case.

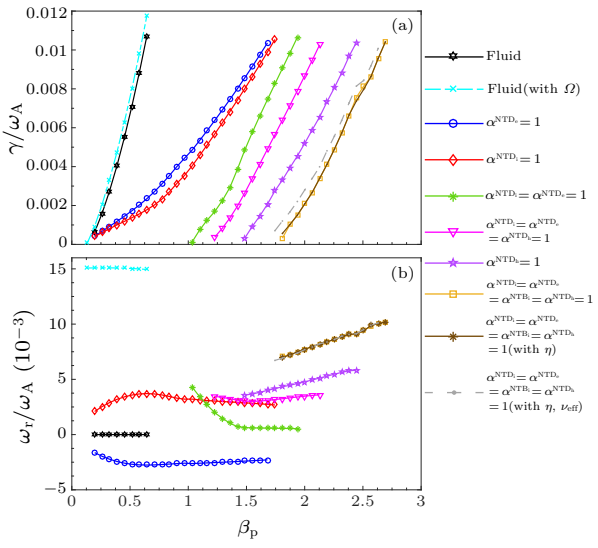

Fig. 7. The growth rate (a) and real frequency (b) of the internal kink mode versus poloidal bata (β_p) with different kinetic effects. A uniform toroidal plasma rotation frequency (normalized by the Alfvén frequency) with $\Omega = 3 \times 10^{-3}$ is assumed. The plasma resistivity, corresponding to Lundquist number $S = 10^{-7}$, is estimated. A simple Krook collision model is assumed for ν_{eff} with both thermal ion collision frequency $\nu_i = 2.2 \times 10^{-4}$ and thermal electron collision frequency $\nu_e = 1.892 \times 10^{-2}$. The collision frequencies are normalized by the Alfvén frequency.

Interestingly, with considering NTD_i and NTD_e simultaneously (green), the mode instability is weakened, and it is worth noting that the value of β_p^{crit} increases to 1. A further additional NTB_i raises β_p^{crit} to 1.2. A comparable result can be seen such that if only NTD_h is included (purple), internal kink will be significantly stabilized, and β_p^{crit} will be increased to 1.5. Meanwhile, when more kinetic effects are added, such as $\alpha^{NTD_i} = \alpha^{NTD_e} = \alpha^{NTD_h} = 1$ (magenta) and $\alpha^{NTD_i} = \alpha^{NTD_e} = \alpha^{NTD_h} = \alpha^{NTB_i} = 1$ (yellow), there exists more stronger stabilization effect on mode, which results in the larger β_p^{crit}. Here, we point out that the plasma resistivity (brown), whose value is realistic and comparable to experimental value on HL-2A, has little impact on mode eigenvalue and β_p^{crit}. The plasma collisionality (gray) has a slight-stabilization effect on internal kink mode. The results shown above may provide an additional insight relevant to the internal kink instability suppression or control.

In summary, we have carried out the synergistic influences of kinetic effects from thermal particles and fast ions on internal kink mode. It is shown that the mode can not be fully stabilized by thermal particles, while it is fully stabilized by fast ions. Meanwhile, the stabilization effects can be significantly enhanced by combined influences from thermal particles and fast ions. The above enhancement results in the remarkable increase of critical value of poloidal beta for driving internal kink. In addition, it is shown that the mode structure is modified by particles' kinetic contributions, especially at the $q = 1$ rational surface, which may have different influences on fast ion transport compared with the standard internal kink. The influence of kinetic internal kink on fast ion transport and loss will be studied in future.

For ITER 15 MA scenario, the internal kink and sawtooth control is an essential issue. Understanding the particles' kinetic effect on internal kink instability is important to estimate the instability behaviors for the ITER device. The synergistic influence of thermal particles and fast ions generated by auxiliary heating and fusion reacting on the internal kink is worthy to study for energetic particle issue.[27]

Acknowledgments. Y. T. Miao would like to acknowledge Dr. T. T. Wu and Dr. X. Bai for their stimulating exchanges and discussions. The author also thank Dr. L. M. Yu and Dr. T. B. Wang for providing experimental data.

References

[1] von Goeler S, Stodiek W and Sauthoff N 1974 *Phys. Rev. Lett.* **33** 1201
[2] Shafranov V D *et al.* 1970 *Sov. Phys. Tech. Phys.* **15** 175
[3] Bussac M N, Pellat R, Edery D and Soule J L 1975 *Phys. Rev. Lett.* **35** 1638
[4] Coppi B, Galvao R, Pellat R, Rosenbluth M and Rutherford

P 1995 *Phys. Plasmas* **2** 533
[5] Porcelli F, Boucher D and Rosenbluth M N 1996 *Plasma Phys. Control. Fusion* **38** 2163
[6] Gibson A, Sekiguchi T, Lackner K, Bodner S and Hancox R 1987 *Nucl. Fusion* **27** 481
[7] White R B, Rutherford P H, Colestock P and Bussac M N 1988 *Phys. Rev. Lett.* **60** 2038
[8] Hastie R J, Hender T C, Carreras B A, Charlton L A and Holmes J A 1987 *Phys. Fluids* **30** 1756
[9] Editors I P B 1999 *Nucl. Fusion* **39** 2137
[10] Liu C, White R B and Rosenbluth M N 1984 *Phys. Rev. Lett.* **52** 1122
[11] White R B, Chen L, Romanelli F and Hay R 1985 *Phys. Fluids* **28** 278
[12] Coppi B and Porcelli F 1986 *Phys. Rev. Lett.* **57** 2272
[13] Coppi B, Migliuolo S and Porcelli F 1988 *Phys. Fluids* **31** 1630
[14] Cheng C Z 1990 *Phys. Fluids B: Plasma Phys.* **2** 1427
[15] Porcelli F 1991 *Plasma Phys. Control. Fusion* **33** 1601
[16] Betti R and Freidberg J P 1993 *Phys. Rev. Lett.* **70** 3428
[17] Shi P W, Chen W and Duan X R 2021 *Chin. Phys. Lett.* **38** 035202
[18] Hu B, Betti R and Manickam J 2006 *Phys. Plasmas* **13** 112505
[19] Miao Y T *et al.* 2020 *Nucl. Fusion* **60** 096022
[20] Liu Y Q, Chu M S, Chapman I T and Hender T C 2008 *Phys. Plasmas* **15** 112503
[21] Antonsen T M Jr and Lee Y C 1982 *Phys. Fluids* **25** 132
[22] Berkery J W, Sabbagh S A, Betti R, Bell R E, Gerhardt S P, LeBlanc B P and Yuh H 2011 *Phys. Rev. Lett.* **106** 075004
[23] Xu M *et al.* 2019 *Nucl. Fusion* **59** 112017
[24] Wu T T, Liu Y Q, Liu Y, Zhou L N and He H D 2019 *Phys. Plasmas* **26** 102102
[25] Liu Y Q *et al.* 2014 *Phys. Plasmas* **21** 056105
[26] Antonsen T M and Bondeson A 1993 *Phys. Fluids B: Plasma Phys.* **5** 4090
[27] Chen W and Wang Z X 2020 *Chin. Phys. Lett.* **37** 125001